AAEC/TM592

AUSTRALIAN ATOMIC ENERGY COMMISSION

RESEARCH ESTABLISHMENT
LUCAS HEIGHTS

AN INVESTIGATION OF THE MEASUREMENT OF VOID-FRACTION IN AIR-WATER MIXTURES BY THE ELECTRICAL IMPEDANCE METHOD

by

G.J. CYBULA

June 1971

ISBN 0 642 99429 3

AUSTRALIAN ATOMIC ENERGY COMMISSION

RESEARCH ESTABLISHMENT

LUCAS HEIGHTS

AN INVESTIGATION OF THE MEASUREMENT OF VOID-FRACTION IN AIR-WATER MIXTURES BY THE ELECTRICAL IMPEDANCE METHOD

by

G.J. CYBULA

ABSTRACT

An impedance type void meter is described which is suitable for measurement of void-fraction in air-water and steam-water mixtures. The mechanical construction of the meter differs from those previously described in that it minimises problems with pressure casing penetrations and with sealing of connecting leads.

A condensed theoretical analysis of the behaviour of the meter in air-water mixtures is included, together with a discussion of possible errors due to changes in conductivity of water and excitation frequency.

Two different systems of electronics are described, a series and a bridge type system.

An experimental calibration of the prototype meter by the "quick-closing valves method" is compared with the theoretical response and the disagreement arising from the comparison is explained.

National Library of Australia card number and ISBN 0 642 99429 3

CONTENTS

continued ...

CONTENTS (continued)

1. INTRODUCTION

Heat transfer work on the performance of water cooled reactor fuel assemblies often demands some knowledge of steam quality at the exit of the assembly. The steam quality (X) is defined by

$$X = \frac{A_v G_v}{A_v G_v + A_\ell G_\ell}$$

where A_v = cross-sectional area of gaseous phase
G_v = mass velocity of gaseous phase
A_ℓ = cross-sectional area of liquid phase
G_ℓ = mass velocity of liquid phase.

Also $G_v = V_v \rho_v$

where V_v = velocity of gaseous phase
ρ_v = density of gaseous phase.

Similarly $G_\ell = V_\ell \rho_\ell$.

The steam quality so defined takes into account slip (S) and void fraction (α), where

$$S = \frac{V_v}{V_\ell} ,$$

V_v = velocity of vapour
V_ℓ = velocity of liquid

and

$$\alpha = \frac{A_v}{A_v + A_\ell}$$

and is related to them by

$$X = \frac{S\alpha\rho_v}{(1 - \alpha)\rho_\ell + S\alpha\rho_v} .$$

It is difficult to measure X directly with reasonable accuracy. However an estimate can be made, since α can be measured by many methods with acceptable accuracy, and S can be measured by noise analysis techniques (Carrard and Ledwidge 1971).

The principles of impedance methods of voidage measurement are well known (see references).

The work reported here aimed to develop an instrument which could be used to monitor α continuously in a high temperature and pressure water environment out-

of-pile. It was also envisaged that it could be adapted for use in in-pile instrumented fuel assemblies, so the void meter itself had to satisfy some stringent requirements. In particular, it should withstand high internal pressures without possibility of leakage, its insulation should not deteriorate due to moisture or high temperature, and electrical connection leads should not present any pressure sealing problems.

2. LITERATURE SURVEY

A detailed literature search showed that a design of an impedance type void meter satisfying the above requirements had not been produced.

For example, Zuber and Findlay (1965) provided only a good analysis and a general method for interpreting experimental data. Sakurai et al. (1964) described a capacitance type void meter. However, most writers agree that this method is sensitive to void distribution (see Orbeck 1964), and poses some problems with capacity of connecting leads.

Lafferty et al. (1967) discuss a conductivity probe which measures local void fraction at a point along a radius or diameter of a channel. Clearly this method does not give an instantaneous average indication of void fraction across the whole cross-section of a channel.

Olsen (1967) gives a most thorough theoretical analysis and provides experimental data from a number of prototypes of different design. Only two were suitable for high temperature work, but both could be used only inside another pressure casing, that is, they could not contain pressure within their own casing. These designs were unsuitable for our purpose.

The void meter used by Akeson (1968) produced an inhomogeneous electric field due to its crossed-plate construction. Olsen (1967) showed that an inhomogeneous field gives rise to large systematic errors in the output signal. This void meter used only one external connection which had to penetrate a pressure tube.

Schenk (1967) and Orbeck (1964) used impedance void meters in-pile for a number of years. They achieved a large measure of success with design and in-pile calibration and performance. However, moisture entering lead insulation at sealing points caused a large failure rate. This was partly solved by using a bare lead insulated with ceramic sleeves and brought out through a sealing gland at the top of the fuel element. The electrode plates in their designs were supported on ceramic insulators which penetrated the outer casings of the void meters. We considered this undesirable for our purpose.

In seeking to design a new type of void meter we have carried out development, testing and calibration in air-water mixtures on the assumption that the behaviour of the meter will be similar in steam and water.

3. THEORY OF THE CONDUCTIVITY METHOD

If two metal plates each of area A and with separation d are immersed in water and an a.c. voltage is applied as shown in Figure 1a the water will present an impedance to the flow of current. The equivalent circuit of such a system is shown in Figure 1b, where

R = resistance due to conductivity of the water
C_s = capacitance due to polarisation of water molecules at each plate
C_p = capacitance with water as dielectric.

Since replacement of some of the water between the plates by air will vary the impedance, this provides a measure of the void fraction. The expression for the total impedance of the system will contain ω, R, C_s and C_p. With the exception of ω, each is a variable depending on the physical conditions between the plates at any given time. These conditions are the geometry of the plates, temperature, types of ions present, ionic concentration, and dielectric constants.

If the geometry of the void gauge is fixed then

$$R = f(\sigma_w, \alpha)$$
$$C_p = f(\epsilon_w, \alpha)$$
$$C_s = f(\epsilon_w, \omega)$$

where σ_w = conductivity of water
ϵ_w = dielectric constant of water.

Therefore, measurement of either R or C_p can indicate void fraction. We selected R as the parameter representing void fraction, and the contributions due to variations in C_p and C_s were minimised.

To gain insight into the behaviour of the void meter at various excitation frequencies, water conductivities and void fractions, the expressions for R, C_s, C_p and $|Z|$ were formulated for a void meter of fixed geometry. These expressions were then programmed for computer calculation of numerical values for the parameters at varying operating conditions.

3.1 Minimising Contributions from C_s and C_p

The equivalent circuit (Figure 1b) can be successively modified as in Figures 1c and 1d provided that the branch containing C_s' and R' (Figure 1c) in parallel has the same impedance as the corresponding branch (Figure 1b) with C_s and R in series. Equating the admittances of the branches, we have

$$\frac{1}{R + \frac{1}{j\omega C_s}} = \frac{1}{R'} + j\omega C_s' \quad .$$

Rationalising the left hand side,

$$\frac{\omega^2 C_s^2 R}{1 + \omega^2 C_s^2 R^2} + j\omega \frac{C_s}{1 + \omega^2 C_s^2 R^2} = \frac{1}{R'} + j\omega C_s' \quad .$$

Equating real and imaginary parts,

$$\frac{1}{R'} = \frac{\omega^2 C_s^2 R}{1 + \omega^2 C_s^2 R^2} = \frac{1}{R + \frac{1}{\omega^2 C_s^2 R}} \qquad \ldots(1)$$

and

$$C_s' = \frac{C_s}{1 + \omega^2 C_s^2 R^2} = \frac{\frac{1}{\omega^2 C_s}}{R^2 + \frac{1}{\omega^2 C_s^2}} \quad . \qquad \ldots(2)$$

In Equation (1),

$$\frac{1}{R'} \rightarrow \frac{1}{R}$$

when

$$R \gg \frac{1}{\omega C_s} \quad .$$

This can be achieved by:

(i) making R greater (adjusting geometry of gauge and conductivity of fluid),

(ii) making ω greater (using higher frequency), noting that C_s is a function of frequency also,

(iii) making C_s greater (increasing the area of electrodes by geometry or platinising).

Then $R' \simeq R$

and $C_s' \rightarrow 0$.

3.2 <u>The Series Capacitance (C_s)</u>

The presence of the series capacitance C_s is due to the polarisation of the layer of water on the plates of the void gauge. It is assumed that the water layer is of molecular thickness and is present at any void fraction. To substitute a capacitor for the polarisation effect, or the electrode effect as it is often

called, is a considerable simplification. For a fuller explanation of this effect see Olsen (1967). It is sufficient to say here that the equivalent impedance due to the electrode effect is independent of void fraction, strongly dependent on frequency and material in the electrodes, and to some extent dependent on water velocity and temperature. Figure 2 shows the relationship between the capacitance C_s and frequency based partly on measurement and partly on theory. The reactance due to C_s is shown in Figure 3, its actual values being of the order of ohms. Since this is quite small when compared with the values of R of hundreds of ohms, the influence of C_s on the response of the gauge is not very significant.

3.3 The Parallel Capacitance (C_p)

The electrode plates of the void meter with the dielectric fluid between them form a capacitor (C_p), whose value is given by

$$C_p = \frac{\epsilon A}{d} \quad ,$$

where

$$\frac{A}{d} = \frac{1}{\text{Gauge constant}} \quad ,$$

$$\epsilon = \epsilon_r \epsilon_o$$

and ϵ_r = dielectric constant of the medium between the plates,

ϵ_o = permittivity of free space

= 8.85×10^{-14} farad cm^{-1} .

The dielectric constant of water at 30°C is

$$\epsilon_w \simeq 80$$

and for air

$$\epsilon_a = 1.0006$$

Maxwell (1881) gave an expression for a dielectric constant of a homogeneous mixture of two media each having known dielectric constant as:

$$\frac{\epsilon_r - \epsilon_w}{\epsilon_r + 2\epsilon_w} = \alpha \frac{\epsilon_a - \epsilon_w}{\epsilon_a + 2\epsilon_w}$$

which gives ϵ_r at any void fraction (α). Substituting the numerical values for ϵ_w and ϵ_a, we obtain

$$\epsilon_r = 160 \times \frac{1.019 - \alpha}{2.038 + \alpha}$$

and

$$\epsilon = \epsilon_r \epsilon_o = 1.416 \times 10^{-11} \times \frac{1.019 - \alpha}{2.038 + \alpha} \quad \text{farad cm}^{-1} \quad .$$

The change in C_p with varying α can be seen by considering the ratio

$$\frac{C_p}{C_{p,\alpha=0}} = \frac{\epsilon \frac{A}{d}}{\epsilon_{\alpha=0} \frac{A}{d}} = \frac{\epsilon}{\epsilon_{\alpha=0}} = 2 \times \frac{1.019 - \alpha}{2.038 + \alpha} \quad ,$$

where C_p = value of C_p at any α

$C_{p,\alpha=0}$ = value of C_p at $\alpha=0$.

In Figure 4 this ratio is plotted against void fraction. Since it is the reactance due to C_p that is of interest, we can also consider the reactance ratio variation with α. The reactance ratio is calculated from

$$\frac{X_{C_p}}{X_{C_p,\alpha=0}} = \frac{\frac{1}{\omega C_p}}{\frac{1}{\omega C_{p,\alpha=0}}} = \frac{C_{p,\alpha=0}}{C_p} \quad ,$$

where X_{C_p} = reactance due to C_p at any α

$X_{C_p,\alpha=0}$ = reactance due to C_p when $\alpha=0$.

This ratio is plotted in Figure 5.

The equivalent circuit in Figure 1d shows that the reactance due to C_p has a shunting effect on R and should therefore be made large to minimise this effect. This implies a small ω and C_p, which is in conflict with minimising errors due to C_s. A compromise has to be made.

3.4 Effect of Voidage on R

If the space between the plates in Figure 1a is filled with water only, then the resistance (R_w) is

$$R_w = \frac{l\ d}{\sigma_w A}$$

where σ_w = conductivity of water.

If the same space is filled with air only,

then $$R_v = \frac{l\ d}{\sigma_v A}$$

where σ_v = conductivity of air or steam.

For the case where the space contains a mixture of water and air, an expression for the resultant effective conductivity can be obtained from Maxwell's equation (1881). This equation expresses the effective dielectric constant for a medium consisting of two components with different dielectric properties. The measurement is considered to be made between the centre and surface of a sphere filled with a homogeneous mixture of the two components. Assuming an analogy between dielectric constant and conductivity, Maxwell's equation can be used to provide a basis for theoretical predictions about the behaviour of the void gauge, and for comparison with experimental results. Written in terms of conductivities the equation becomes

$$\frac{\sigma - \sigma_w}{\sigma + 2\sigma_w} = \alpha \frac{\sigma_v - \sigma_w}{\sigma_v + 2\sigma_w}$$

where σ = effective conductivity of the mixture.

Since $\frac{\sigma_v}{\sigma_w} \to 0$

then $$\sigma = 2\sigma_w \frac{1 - \alpha}{2 + \alpha} \quad .$$

Thus, if $\alpha = 0$, then $\sigma = \sigma_w$
if $\alpha = 1$, then $\sigma = 0$.

Therefore the effective resistance of a mixture becomes

$$R = \frac{2 + \alpha}{2\sigma_w(1 - \alpha)} \frac{d}{A} \quad .$$

It can be seen that

$$R \to \infty \quad \text{when} \quad \alpha = 1$$
$$R = \frac{1}{\sigma_w} \frac{d}{A} \quad \text{when} \quad \alpha = 0 \quad .$$

If we consider the change in resistance with void fraction, that is, the ratio of resistance at any α to that at $\alpha = 0$, we have

$$\frac{R_\alpha}{R_{\alpha=0}} = \frac{\frac{2 + \alpha}{2\sigma_w(1 - \alpha)} \frac{d}{A}}{\frac{2}{2\sigma_w} \frac{d}{A}} = \frac{2 + \alpha}{2(1 - \alpha)} \quad .$$

Therefore, the fractional change in resistance is a function of α only. In Figure 6 this ratio is plotted against void fraction.

3.5 The Total Impedance of the Void Meter

The modulus of the total impedance $|Z|$ of the void gauge was obtained from

$$|Z| = \left| \frac{(R + X_{C_s})X_{C_p}}{R + X_{C_s} + X_{C_p}} \right| .$$

Again, it should be noted that although the modulus of the impedance is a functio of frequency, water conductivity and void fraction, the ratio of the impedance at any α to the impedance at $\alpha = 0$ is a function of void fraction only. This is shown in Figure 7.

4. DESIGN OF THE VOID METER

The dimensions of the void gauge and selection of materials for its construction were fixed as follows:

(i) Internal diameter = 3.81 cm, fixed by the most common internal diameter of air-water test sections.

(ii) Length = 6.35 cm, fixed by expected frequency response. It was considered more desirable to integrate the measurement over some length of the channel and thus obtain a slow varying output.

(iii) Although steam-water facilities did not exist at the time, it was expected that when constructed, such a facility would operate at up to 140 atm and 260°C. Therefore the outer casing and any joints to the test section pipework should be pressure tight to 140 atm, and any insulation used should be good at 260°C.

(iv) Separation between plates = 0.416 cm, fixed by expected bubble size, internal diameter of void meter, and an attempt to approximate the two-plate theory of the void meter.

Figure 8 shows the longitudinal cross-section of the void meter. The design permits the insertion of the electrode shells from both ends of the pressure casing. Thus there are no penetrations of the casing and therefore no sealing problems.

Figure 9 shows that each electrode shell is a single integral part fully self-supporting with the cylinders welded to the support ribs. Electrical connections are made to the flange of each electrode shell on the outside of the void meter. It should be pointed out that it would be relatively simple to dispense with one flange, by fixing one electrode shell permanently in a metal pipe, and insulating the other shell. In this way, only one electrical connection would be needed, the other being common with all the pipework.

4.1 Gauge Constant

The gauge constant was calculated from the dimensions of the void gauge (or void meter) as

$$\frac{d}{A} = 2.5 \times 10^{-3} \text{ cm}^{-1}$$

where d = distance between plates

A = area of one plate,

= area of all the individual cylinders connected to one terminal.

By immersing the gauge in a fluid held at a known constant temperature and conductivity and measuring the resistance between the shells, the gauge constant was found to be

$$\frac{d}{A} = 8.126 \times 10^{-3} \text{ cm}^{-1} \quad .$$

The measured value was used in preference to the calculated value of $\frac{d}{A}$ since it is more representative of the true conditions existing when the void meter is mounted in a test channel and fringing effects take place.

5. EXPERIMENTAL CALIBRATION OF THE VOID METER

Figure 10 is the flow diagram of a facility which supplies the void meter with air-water mixtures. Its salient features are:

(i) Water circulation from 0 to 1.137×10^{-3} m^3 sec^{-1}, with water temperature control from ambient to 40°C.

(ii) Water by-pass to a deionising column, with continuous conductivity control and indication.

(iii) Air supply from 0 to 4.72×10^{-3} m^3 sec^{-1} continuously variable, with a heating facility so that air temperature can be made equal to water temperature.

(iv) A 2.34 m length of transparent and graduated pipe, with two pneumatically operated quick-closing valves, one at either end of the pipe, for independent void fraction measurement.

(v) An air-water mixer consisting of a porous bronze sleeve, through which the air is forced into the water.

(vi) Air and water flow measuring instruments of the float and turbine type.

5.1 Voidage Read-out Circuits

To convert the change in resistance of the void gauge to a voltage or current proportional to void fraction several circuits were tried. Of the more successful ones only the series and a.c. bridge circuits are described here.

5.1.1 Series circuit

Figure 11 is a schematic diagram of the series circuit. The a.c. amplifier supplies approximately 1 watt of a.c. power to the void gauge. Since the impedance of the void gauge changes with void fraction the applied voltage must be adjusted at

point A (w.r.t. earth) to one constant value before calibration. This is achieved by adjusting the 5k Ω shunting resistor. In a practical instrument an automatic gain control circuit on the a.c. amplifier could be used in place of the 5k Ω resistor. Thus if the voltage across the A to E branch is kept constant, then as the resistance of the void-gauge changes, the current through R_s will change, producing a changing voltage drop across R_s. This voltage drop, being proportional to void fraction, is rectified and may be measured on a d.c. voltmeter or recorded.

5.1.2 a.c. bridge circuit

The a.c. bridge circuit, shown in Figure 11, utilises a compensating gauge which is inserted into a region where only water flow is present at all times. If this bridge is balanced for zero output when only water flows through both the compensating and the void gauge, then any output which appears when air is inserted into the water before the void gauge, will be due to void fraction only. Influences due to conductivity or temperature changes are minimised by the compensating gauge. The gauge constant ($\frac{d}{A}$) of the compensating gauge should be approximately equal to the gauge constant of the void gauge. This technique has been used, with good results, in the experiments described here.

5.2 Calibration

The void gauge was calibrated by the quick-closing valves method in which two simultaneously closing valves trap a portion of the two-phase flow in a long pipe of uniform internal diameter. After separation of the two phases (air and water) the heights of the air and water columns are measured to give void fraction. Figures 12 and 13 show the experimental results, and the theoretical curves from the Maxwell formula for conductivity of a homogeneous mixture.

To obtain a measurement of utmost accuracy for any one point on the experimental curve, the void fraction was set to the required value, the conductivity and temperature were allowed to settle at predetermined levels, ten readings were taken, and their mean was plotted.

6. ERRORS

(a) Figure 14 shows a theoretical estimate of error caused by using changes in resistance rather than changes in impedance as an indication of void fraction. It should be pointed out that the changes in resistance have been calculated with the help of Maxwell's expression, which in our case is not in complete agreement with experiment (see Figures 12 and 13). Thus, the representation of error shown in Figure 14 is valid only if it is assumed that Maxwell's expression accurately represents resistance changes due to void fraction. On that assumption, it can be seen that at conductivities greater than 5 $\mu\ \Omega^{-1}\ cm^{-1}$ and frequencies from 1 to 10 kHz, the error caused by considering resistance changes only, will always be less than 0.5 per cent.

It can also be seen that the error increases with increase in frequency, and decreases with increasing conductivity. This figure proves that it is sufficient to consider resistance of the gauge, since all capacitive influences introduce only an insignificant error. The same figure enables the experimenter to choose optimum excitation frequency and water conductivity.

(b) The disagreement between experimental results and Maxwell's theory, shown in Figures 12 and 13, has several causes. Firstly, the geometry of our gauge is such that Maxwell's expression is not exactly applicable. As mentioned in Section 3.4 Maxwell's expression was derived for a spherical configuration where fringing effects do not exist, and electrical field distribution is exactly describable. In the case of our void gauge, fringing effects are very prominent, owing to the finite length of the cylinder electrodes. The distribution of the field is complicated further by the supporting ribs which penetrate the cylinders. This accounts for the large difference between the calculated and measured gauge constants, as well as for the experimental readings being lower than indicated by the Maxwell expression.

The second factor influencing the experimental readings is the moisture content of the air inside the bubbles. The resistance of a "humid" air bubble is much lower than that of a "dry" air bubble. In the Maxwell expression we have assumed an infinite resistance for air. An attempt was made to compare the resistance of moist and dry air in an effort to reduce the discrepancy between the experimental and theoretical results. However, owing to instrument limitations these attempts were largely inconclusive.

Finally, void distribution within the void gauge also influences the experimental results. This was proved by Orbeck (1964) and Olsen (1967). In particular, Olsen found that void distribution in the bubble flow regime had only a negligible effect on the response of the void gauge but, the influence increased with increasing void fraction.

(c) The experimental readings, as plotted in Figures 12 and 13, were taken at an excitation of 6 kHz, and water conductivity of 20 $\mu\ \Omega^{-1}\ cm^{-1}$. Mixing of air and water was good up to about 30 per cent void fraction and the size of the bubbles remained fairly constant within the range 1 to 4 mm. At higher void fractions large pockets of air appeared, gradually forming large slugs. Oscillations of flow follow and it is necessary to introduce a large time constant into the output of the read-out circuit in order to get a sensible average reading. Repeatability tests gave a figure of $\pm$ 3 per cent. The uncertainty here was largely due to instability in the excitation oscillator amplitude and amplifier gain, inaccuracies in temperature and conductivity control, and to a small extent the error due to the quick closing valves.

7. TRANSIENT RESPONSE AND SENSITIVITY

From tests with a very much reduced time constant on the output circuit, and sudden introduction of air into the void gauge, it is estimated that the gauge can easily handle 3 Hz. It should be pointed out that the useful lower limit of the time constant depends on the excitation frequency. Thus low time constants cannot be used with low excitation frequencies.

Sensitivity tests were carried out by introducing very small quantities of air into a constant water flow. The bridge circuit proved to be more suitable than the series circuit in these tests. The detectable quantities of air were so small that the quick closing valves with the 2.34 m length of flow channel between them could not give a measure of void fraction. By a rough estimate it can be said that the void meter will detect a void fraction of 0.01 per cent.

8. DISCUSSION

The void gauge described in this paper could eventually be used in steam-water mixtures where the operating conditions would be quite different to those in air-water. Therefore, it may be appropriate to attempt to predict the behaviour of the impedance gauge in steam and water.

It is generally agreed in the literature that from the point of view of conductivity and dielectric constant, dry steam is similar to air. The conductivity of water increases at approximately 2 per cent per °C in the ambient temperature region, the rate diminishing gradually until the conductivity is nearly constant near 200°C.

Thus, if the gauge operated at approximately 200°C or higher, temperature variations of ± 20°C or more would not introduce significant errors. Changes in conductivity of water due to varying ion concentration would have a detrimental effect on accuracy. However, in any real situation such as a water cooled fuel element assembly, or a steam-water experimental rig, the water conductivity is usually closely controlled.

Therefore, the only difficulty that remains is the calibration of the gauge on steam-water mixtures. The quick closing valve method is difficult, but not impossible, to implement.

Another method utilises two identical turbine flow meters. One flow meter is inserted in the water phase region, the other into the two-phase region. The difference in readings from the two turbines can indicate void fraction.

The impedance void meter appears to be well suited for use in-pile in instrumented fuel assemblies. It can be small and can be designed without any penetrations of the outer casing of the assembly. Only one electrical connection to the outside is needed, since the other plate of the meter can be common with the structure of the assembly.

9. ACKNOWLEDGEMENTS

The author wishes to express gratitude to Dr. R. W. Harris who programmed all the computer work in the theoretical analysis of the void meter.

Thanks are also due to Mr. J. Marshall for his valuable support during the early stages of this work.

10. REFERENCES

Akesson, H. (1968). - Local Void Measurements in Oscillating Two-phase Flow. AE-RTL-1010.

Carrard, G. and Ledwidge, T.J. (1971). - Measurement of Slip Distribution and Average Void Fraction in an Air Water Mixture. A.A.E.C. To be presented at the First International Symposium on Two-phase Systems, Haifa, Israel.

Lafferty, J.F. and Hammitt, F.G. (1967). - A Conductivity Probe for Measuring Local Void Fractions in Two-phase Flow. University of Michigan.

Maxwell, J.C. (1881). - A Treatise on Electricity and Magnetism. Clarendon Press, Oxford, 2nd ed., Vol. 1.

Olsen, H.O. (1967). - Theoretical and Experimental Investigation of Impedance Void Meters. KR-118, Kjeller Report, Institutt for Atomenergi, Norway.

Orbeck, I. (1964). - The Impedance Void Meter for HBWR. HPR-35, OECD Halden Reactor Project, Norway.

Sakurai, Y., Mori, K., Isozumi, K. and Kakizawa, K. (1964). - Capacitance-type Void Meter. Osaka University, Japan.

Schenk, K. (1967). - Development of an In-pile Void Gauge. HPR-75, OECD Halden Reactor Project, Norway.

Zuber, N. and Findlay, J.A. (1965). - Average Volumetric Concentration in Two-phase Flow Systems. Journal of Heat Transfer.

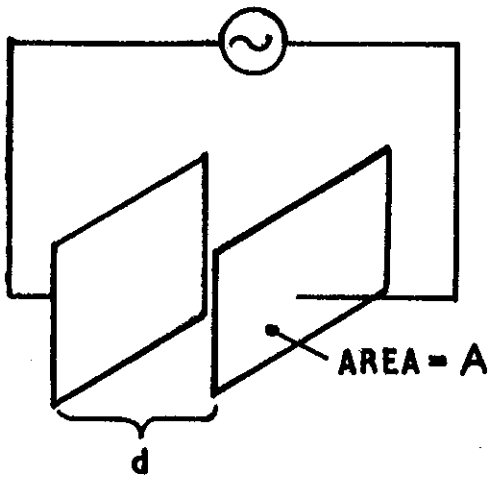

a) A TWO-PLATE VOID METER

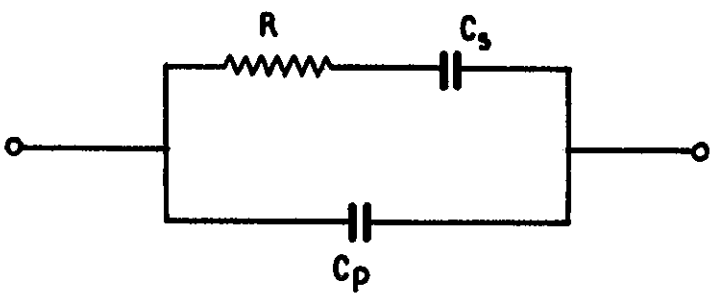

b) EQUIVALENT CIRCUIT OF THE VOID METER

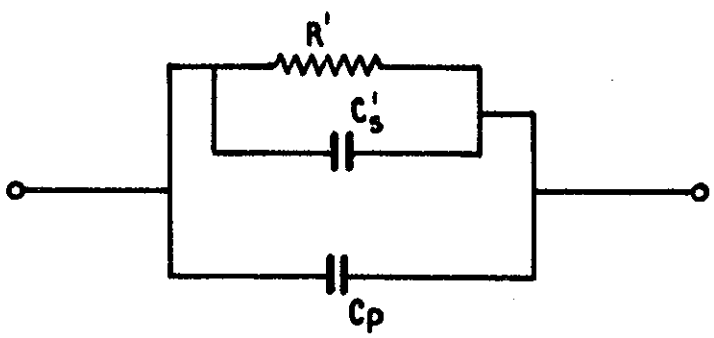

c) REDUCED EQUIVALENT CIRCUIT

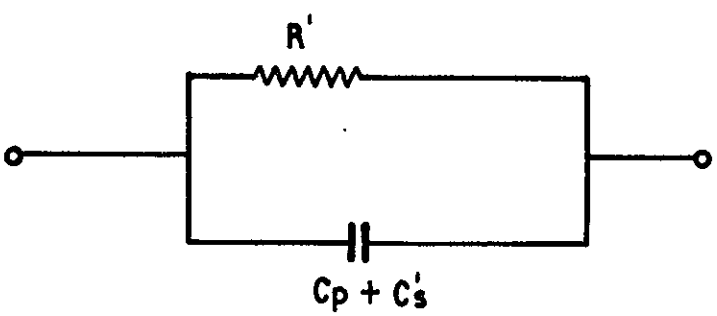

d) FURTHER REDUCTION OF THE EQUIVALENT CIRCUIT

FIGURE 1. EQUIVALENT CIRCUITS FOR A TWO-PLATE VOID METER

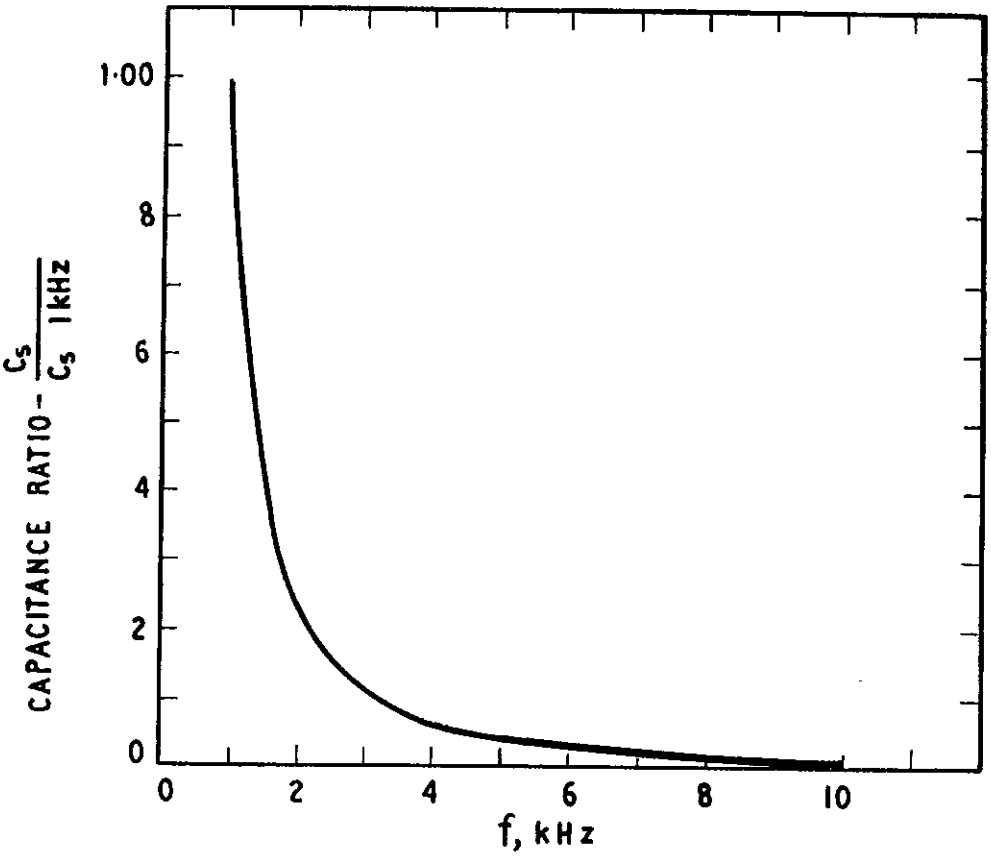

FIGURE 2. SERIES CAPACITANCE VERSUS FREQUENCY

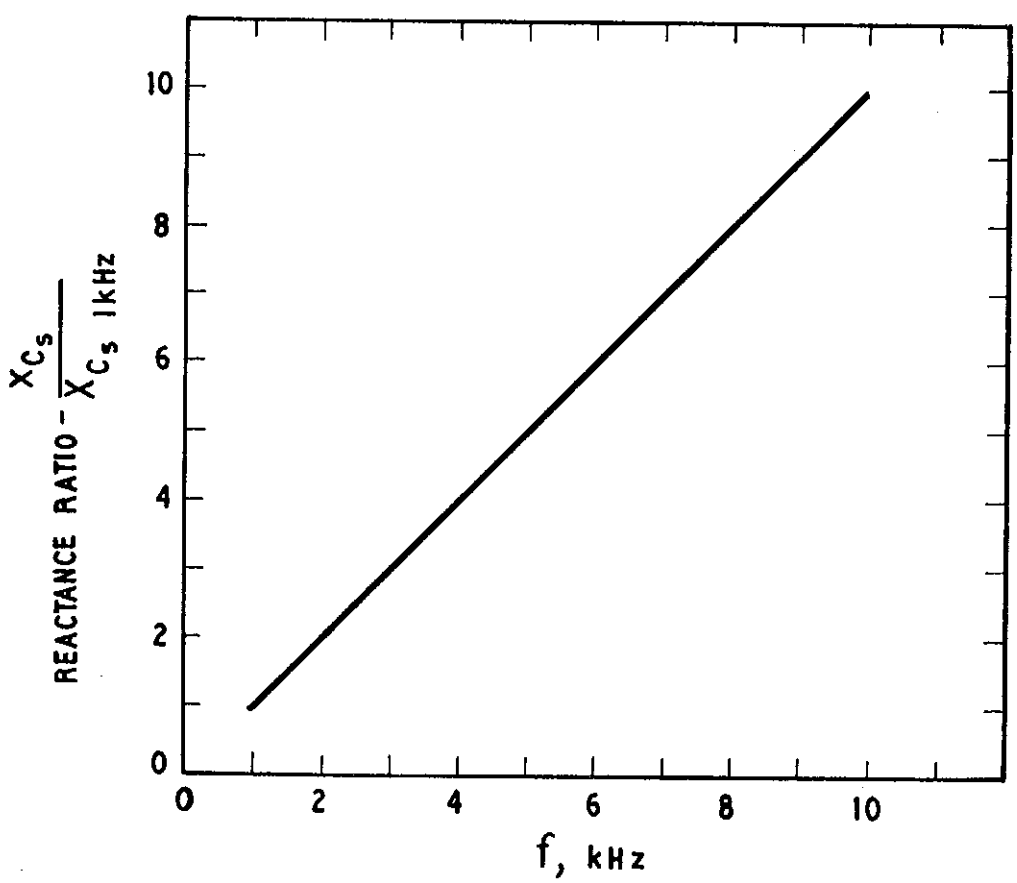

FIGURE 3. REACTANCE DUE TO C_s VERSUS FREQUENCY

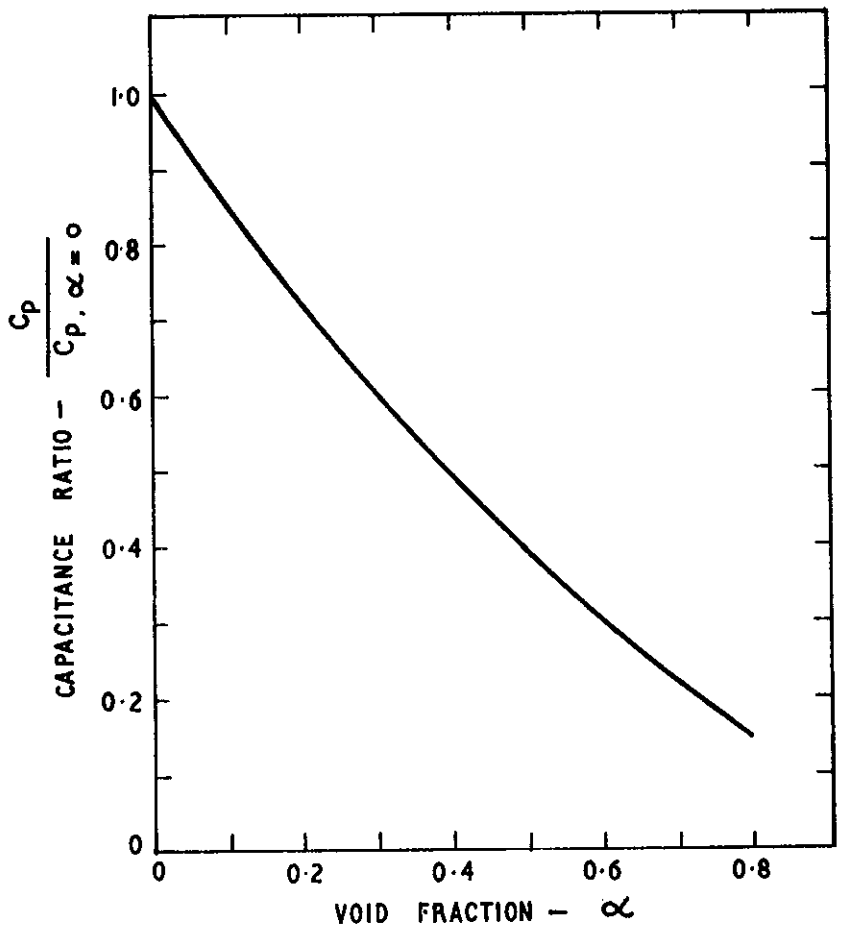

FIGURE 4. THEORETICAL RELATIONSHIP BETWEEN CHANGE IN C_p AND VOID FRACTION

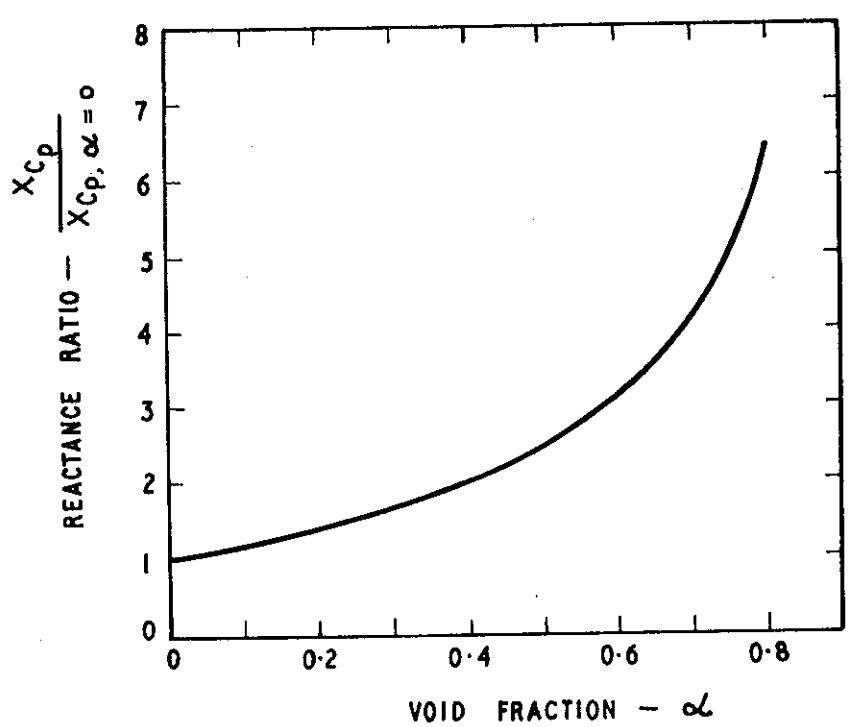

FIGURE 5. THEORETICAL RELATIONSHIP BETWEEN REACTANCE DUE TO C_p AND VOID FRACTION

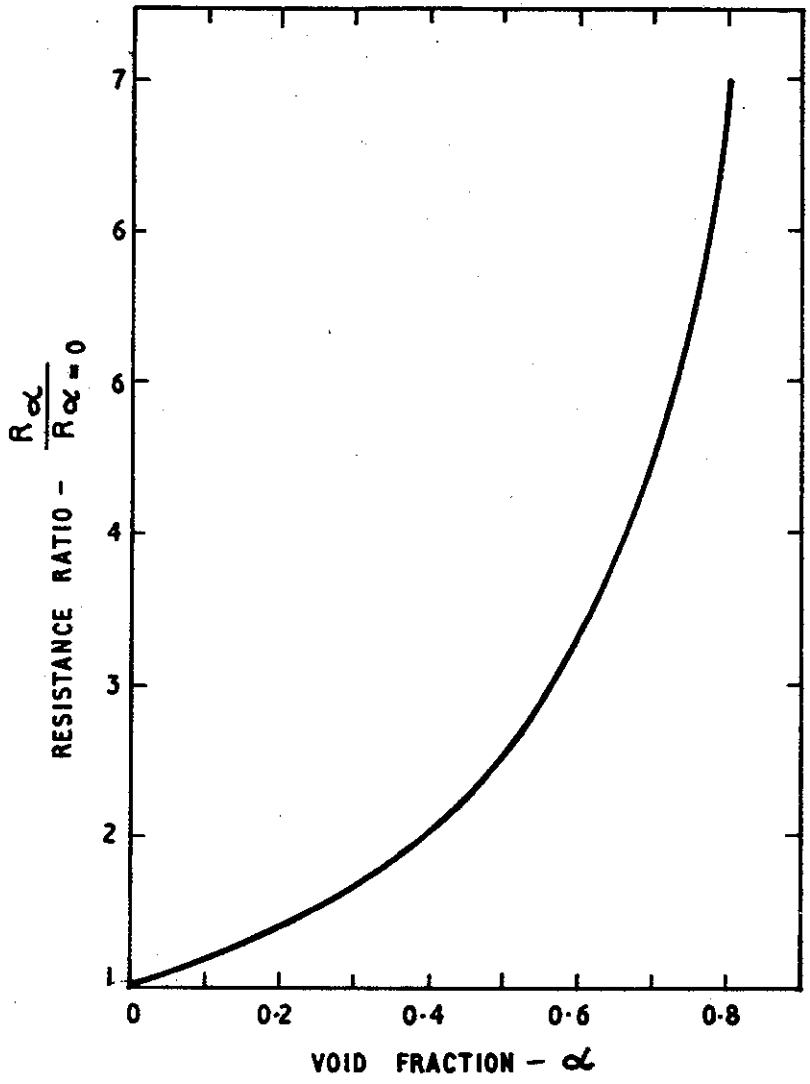

FIGURE 6. MAXWELL RELATIONSHIP BETWEEN $R_\alpha/R_{\alpha=0}$ AND VOID FRACTION

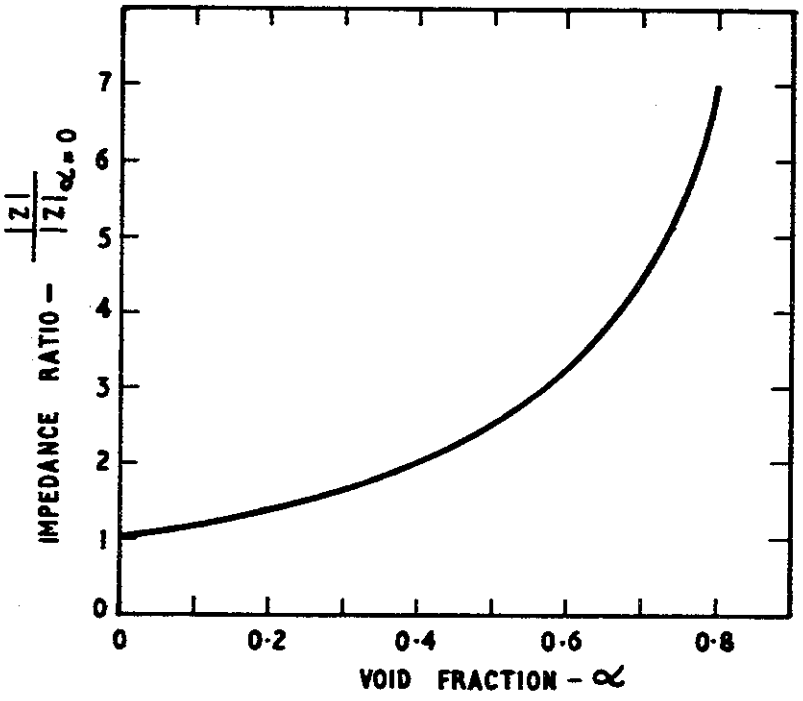

FIGURE 7. THEORETICAL RELATIONSHIP BETWEEN CHANGE IN TOTAL IMPEDANCE AND VOID FRACTION

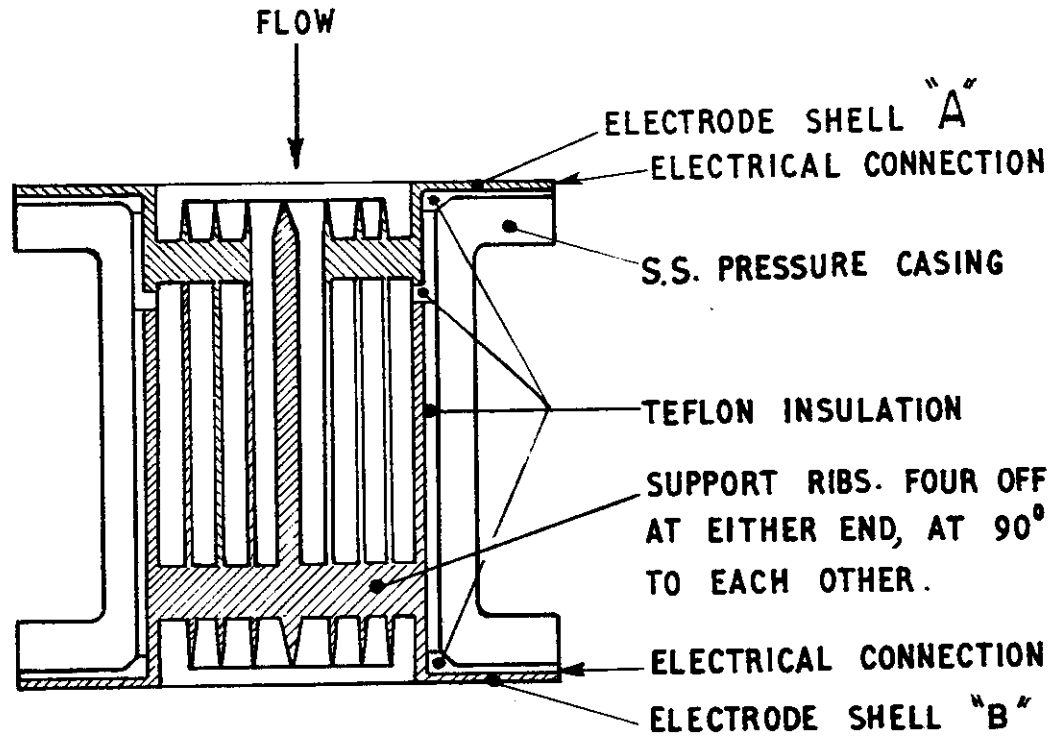

FIGURE 8. LONGITUDINAL CROSS-SECTION OF VOID GAUGE

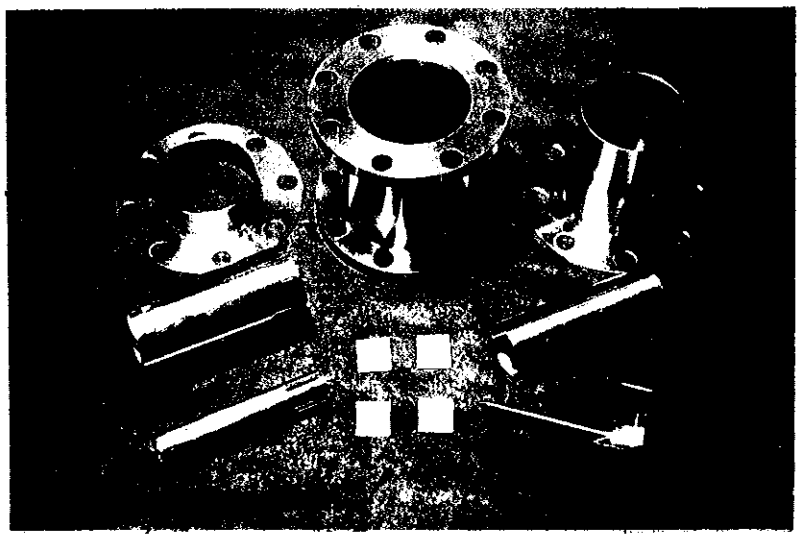

9a. Void meter parts

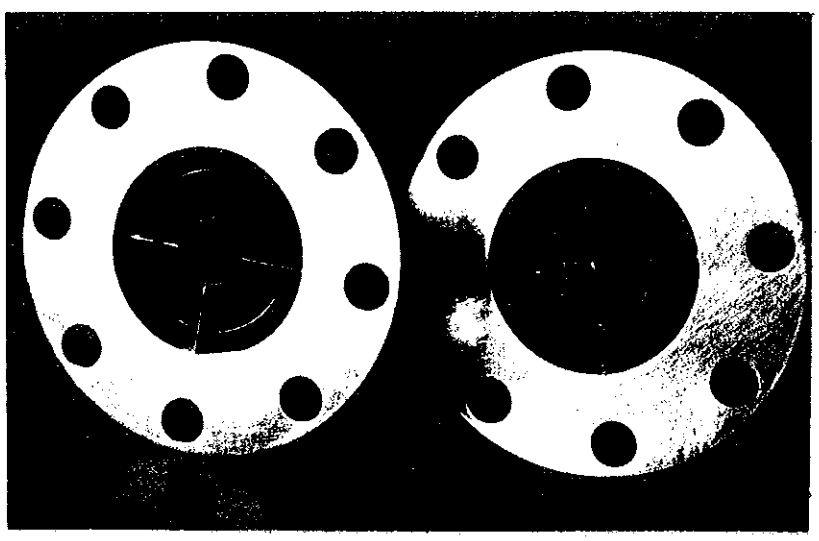

9b. First stage of assembly

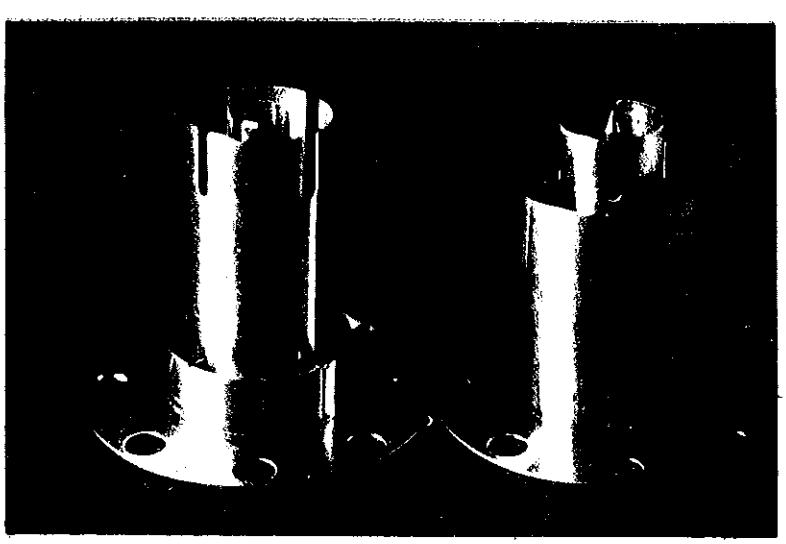

9c. Longitudinal view of electrode shells

FIGURE 9. CONSTRUCTION AND ASSEMBLY OF THE VOID METER

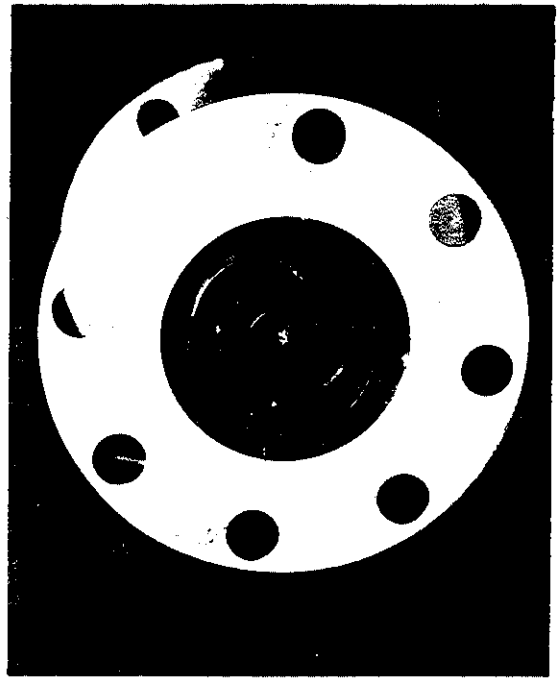

9d. End view of shells, showing method of assembly

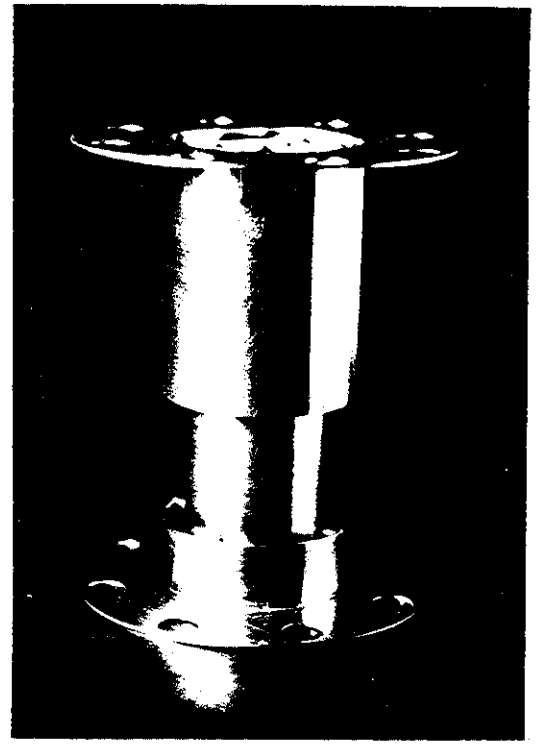

9e. Side view of shells partly assembled

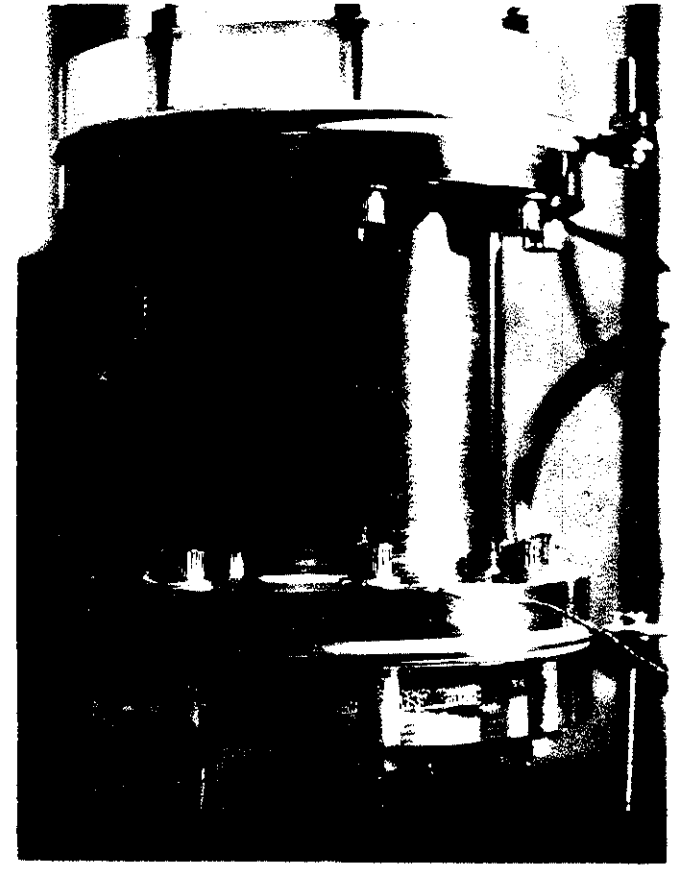

9f. Meter with outer casing assembled and mounted in test section. Note teflon gaskets

FIGURE 9. CONSTRUCTION AND ASSEMBLY OF THE VOID METER

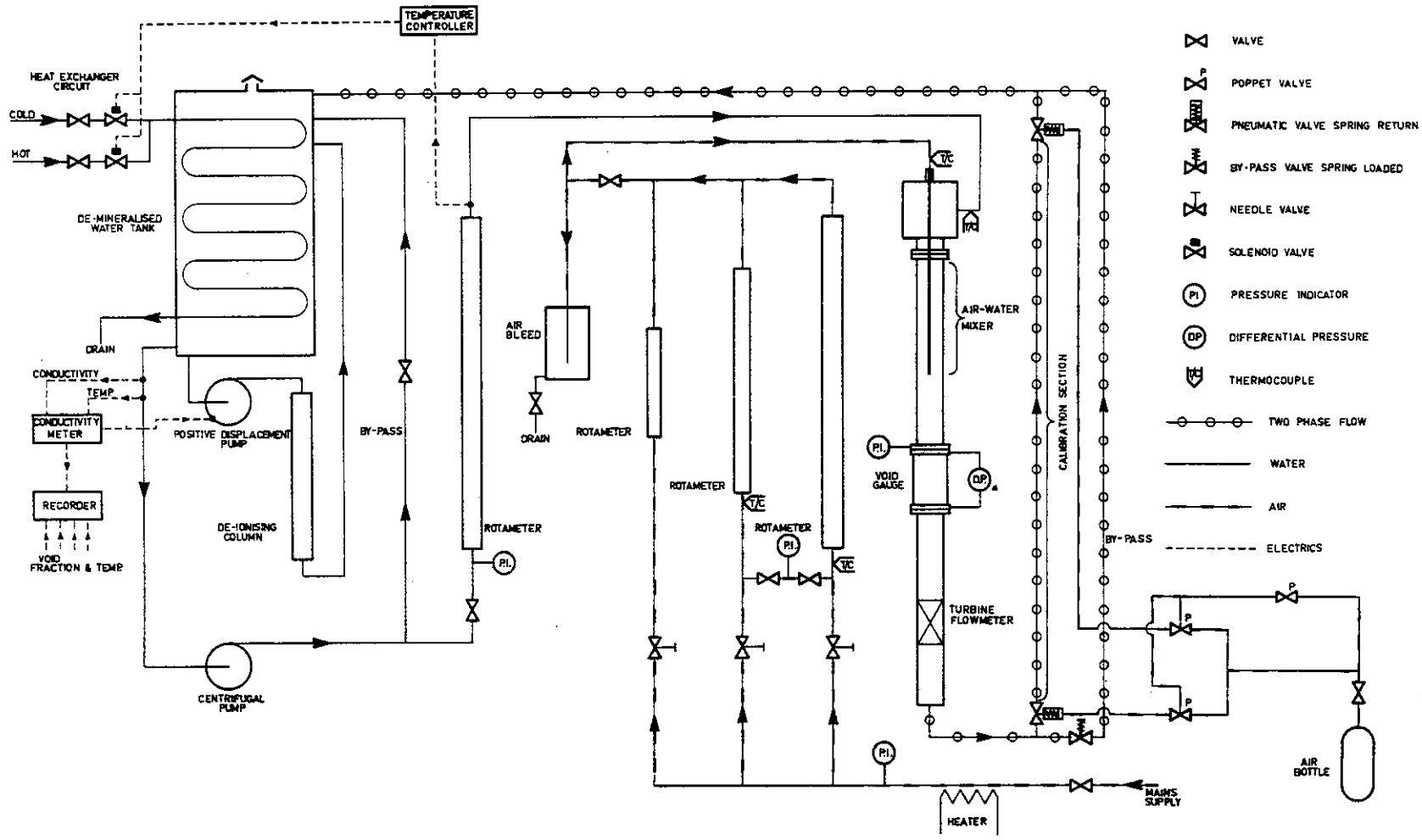

FIGURE 10. FLOW DIAGRAM OF AIR-WATER RIG

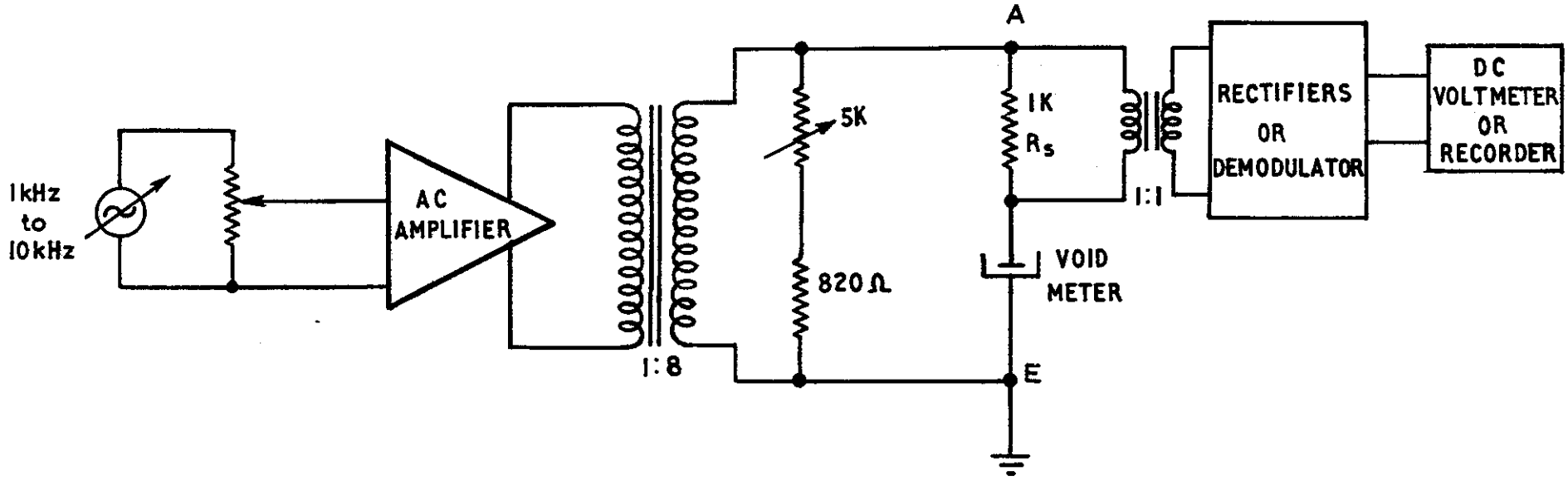

FIGURE 11. VOID METER READOUT CIRCUIT USED IN EXPERIMENTAL CALIBRATION

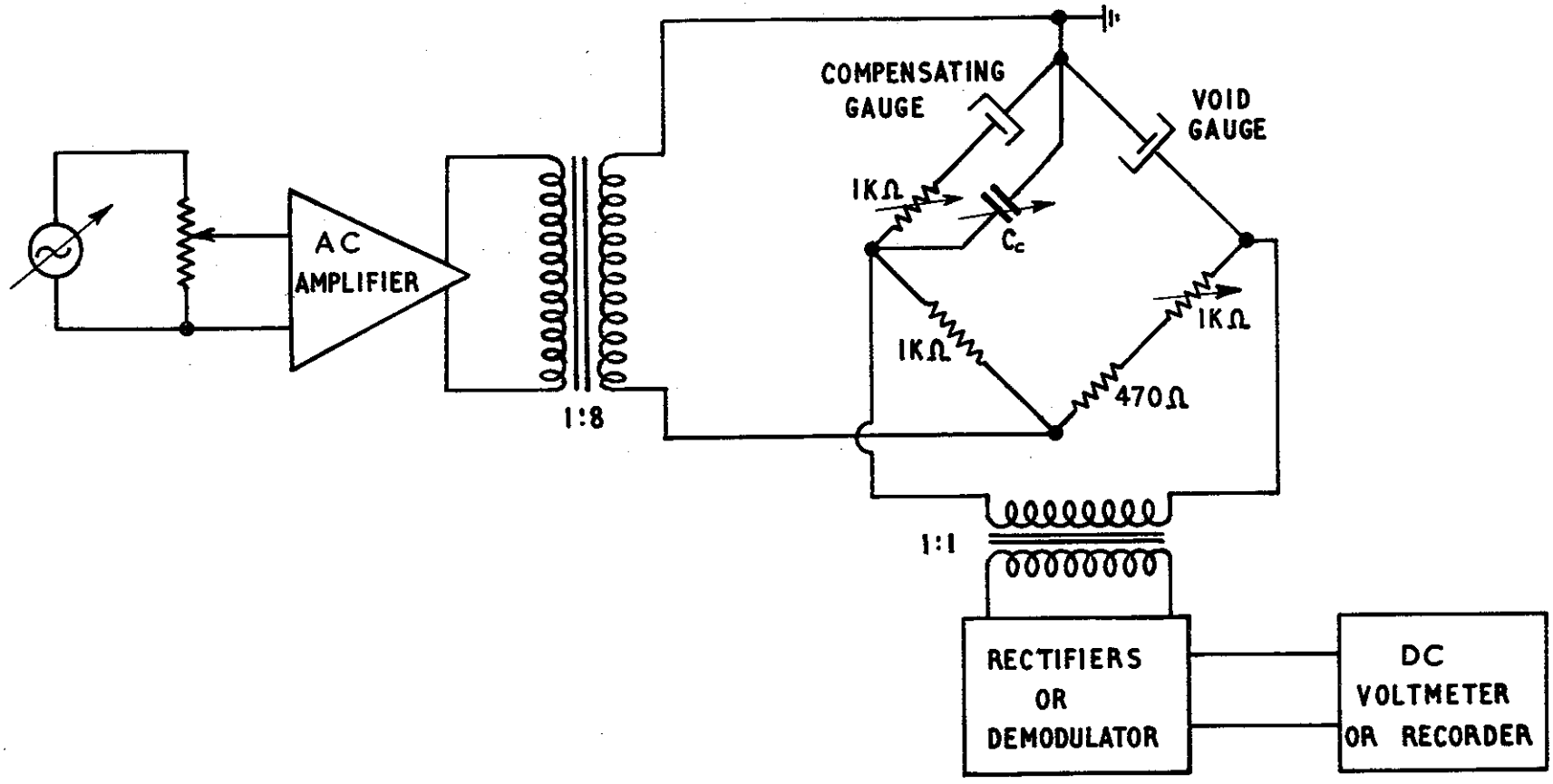

FIGURE 12. A.C. BRIDGE CIRCUIT FOR TESTING THE VOID GAUGE AND COMPENSATING GAUGE

The output signal is due to void fraction only

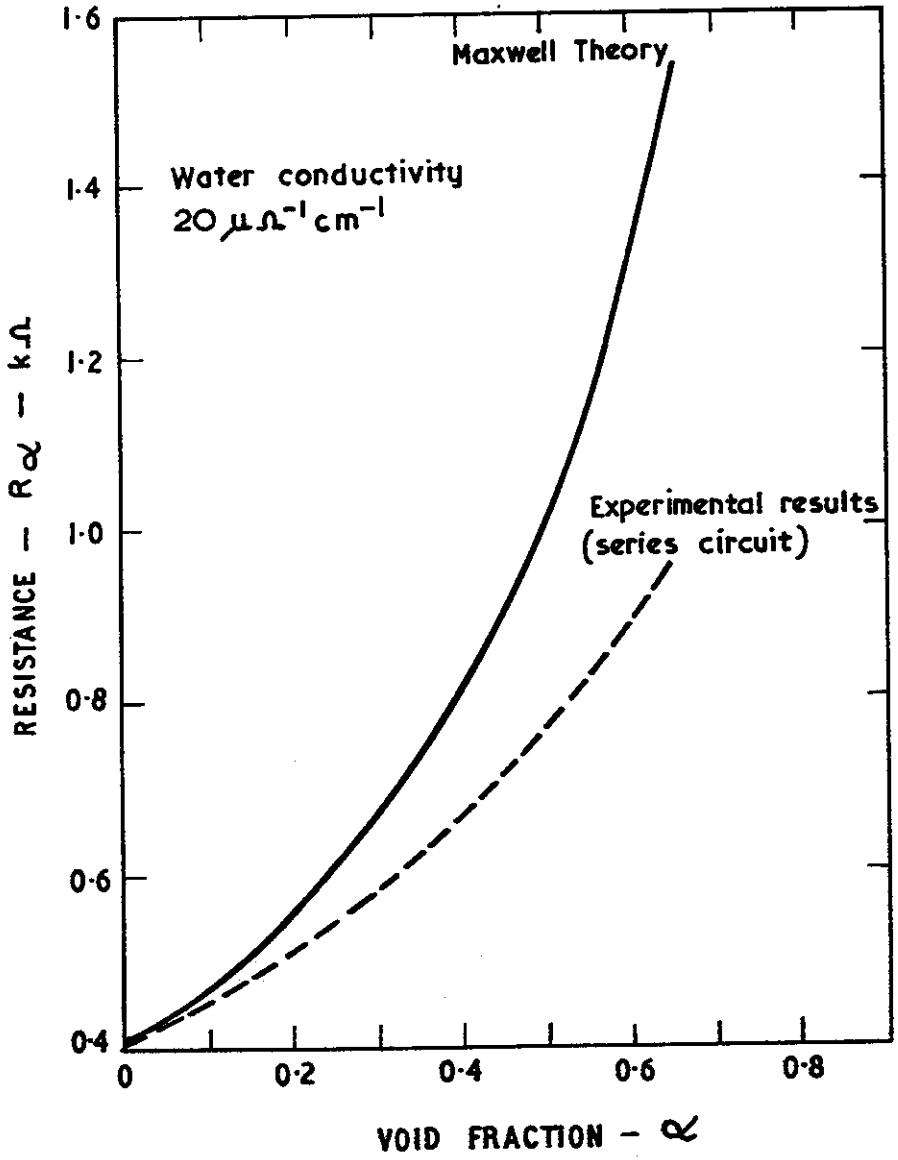

FIGURE 13. RESISTANCE OF GAUGE VERSUS VOID FRACTION

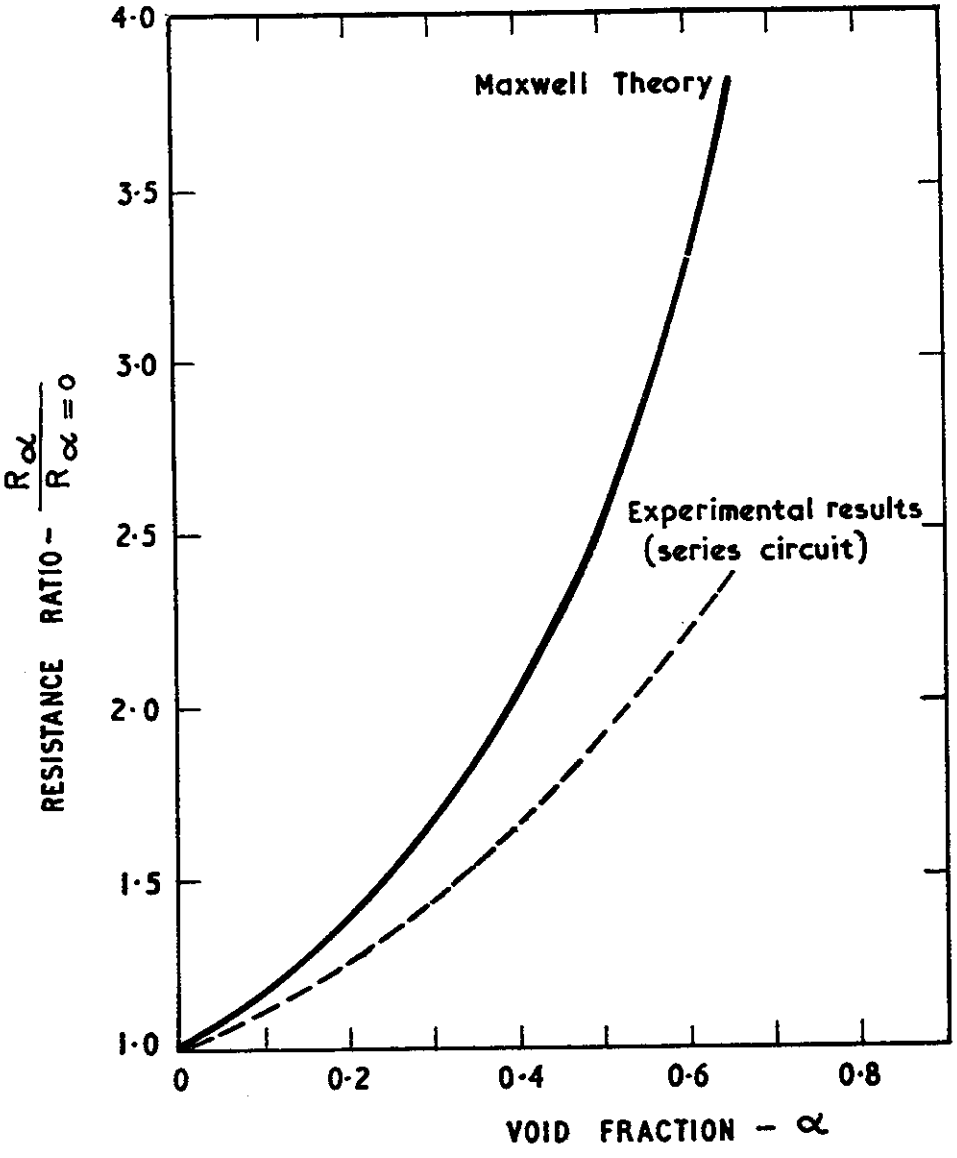

FIGURE 14. COMPARISON OF THEORETICAL AND EXPERIMENTAL CALIBRATION CURVES

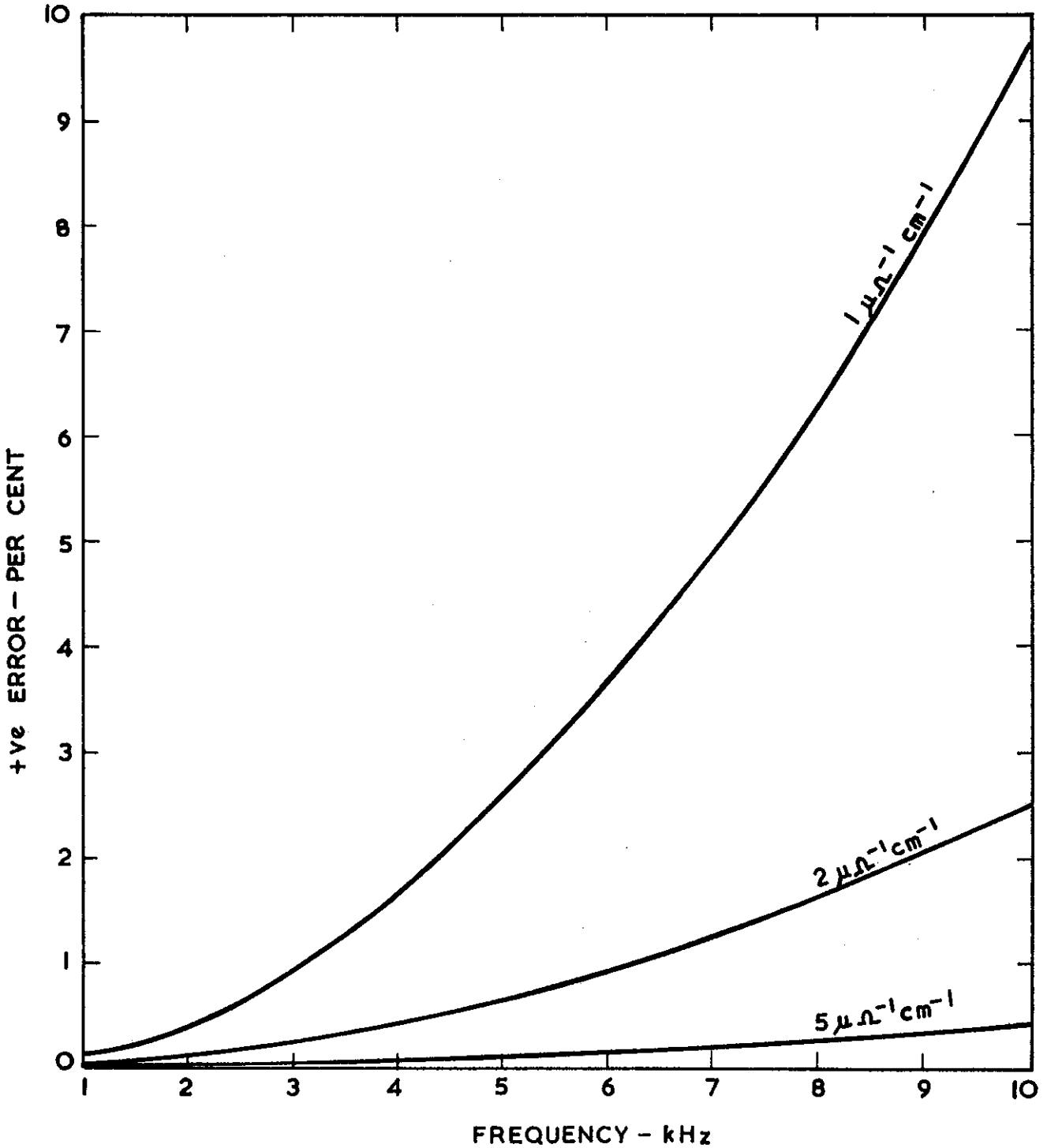

FIGURE 15. FREQUENCY VERSUS ERROR DUE TO CAPACITIVE REACTANCE